Journal of King Saud University – Computer and Information Sciences (2015) 27, 40–45

King Saud University

Journal of King Saud University – Computer and Information Sciences

www.ksu.edu.sa
www.sciencedirect.com

Medical image denoising using dual tree complex thresholding wavelet transform and Wiener filter

Hilal Naimi, Amel Baha Houda Adamou-Mitiche, Lahcène Mitiche *

Science and Technology Department, University of Djelfa, Algeria

Received 7 September 2013; revised 24 December 2013; accepted 13 March 2014
Available online 30 January 2015

KEYWORDS

Discrete wavelet transform;
Stationary wavelet transform;
Wavelet thresholding;
Dual tree complex wavelet transform;
Wiener filter

Abstract Image denoising is the process to remove the noise from the image naturally corrupted by the noise. The wavelet method is one among various methods for recovering infinite dimensional objects like curves, densities, images, etc. The wavelet techniques are very effective to remove the noise because of their ability to capture the energy of a signal in few energy transform values. The wavelet methods are based on shrinking the wavelet coefficients in the wavelet domain. We propose in this paper, a denoising approach basing on dual tree complex wavelet and shrinkage with the Wiener filter technique (where either hard or soft thresholding operators of dual tree complex wavelet transform for the denoising of medical images are used). The results proved that the denoised images using DTCWT (Dual Tree Complex Wavelet Transform) with Wiener filter have a better balance between smoothness and accuracy than the DWT and are less redundant than SWT (StationaryWavelet Transform). We used the SSIM (Structural Similarity Index Measure) along with PSNR (Peak Signal to Noise Ratio) and SSIM map to assess the quality of denoised images.

1. Introduction

The advances of digital imaging technologies include Magnetic Resonance Imaging (MRI), the different digital vascular radiological processes, the cardiovascular and contrast imaging, mammography, diagnostic ultrasound imaging, nuclear medical imaging with Single Photon Emission Computed Tomography (SPECT), Positron Emission Tomography (PET) and multi-detector computed tomography (MDCT). All these processes are producing ever-increasing of images are different from typical photographic images primarily because they reveal internal anatomy as opposed to an image of surface (Rangayyan, 2005), they have revolutionized modern medicine, largely due to technical advances in imaging hardware and new imaging methodologies, the quality of digital medical images becomes an important issue. To achieve the best possible diagnosis it is important that medical images be sharp, clear, and free of noise. Noise removal is essential in medical imaging applications in order to enhance and recover fine details that may be hidden in the data (Satheesh and Prasad, 2011).

* Corresponding author.
E-mail addresses: pgss_2011@yahoo.fr (H. Naimi), amelmitiche@yahoo.fr (A.B.H. Adamou-Mitiche), l_mitiche@yahoo.fr (L. Mitiche).

Peer review under responsibility of King Saud University.

ELSEVIER Production and hosting by Elsevier

http://dx.doi.org/10.1016/j.jksuci.2014.03.015

2. Dual tree complex wavelet transform

Complex Wavelet Transforms (CWT) use complex-valued filtering (analytic filter) that decomposes the complex signals into real and imaginary parts in the transform domain. The real and imaginary coefficients are used to compute amplitude and phase information, just the type of information needed to accurately describe the energy localization of oscillating functions (wavelet basis). Another approach to implement an expansive CWT first applies a Hilbert transform to the data. The real wavelet transform is then applied to both the original data and the Hilbert transformed data, and the coefficients of each wavelet transform are combined to obtain a CWT.

The dual-tree complex wavelet transform (DTCWT) is a relatively recent enhancement to the discrete wavelet transform (DWT), with important additional properties: It is nearly shift invariant and directionally selective in two and higher dimensions. It achieves this with a redundancy factor of only 2^d for d-dimensional signals, which is substantially lower than the Stationary DWT (Selesnick et al., 2005). Extension of the DTCWT to two dimensions is achieved by separable filtering along columns and then rows. However, if both column and row filters suppress negative frequencies, then only the first quadrant of the 2-D signal spectrum is retained. It is well known, from 2-D Fourier transform theory, that two adjacent quadrants of the spectrum are required to represent fully a real 2-D signal. Therefore, in the DTCWT it is also filtered with complex conjugates of the row (or column) filters in order to retain a second (or fourth) quadrant of the spectrum (Kingsbury, 1999).

The dual tree complex DWT of a signal $x(n)$ is computed using two critically-sampled DWTs in parallel to the same data as shown in the following figure (Fig. 1). If the same filters are used in the upper tree and lower tree nothing is gained. So the filters in this structure will be designed in a specific way that the sub bands of upper DWT are interpreted as real part of complex wavelet transform and the lower tree as imaginary part as shown in Fig. 1. The transform is expansive by factor 2 and shift invariant (Naga Prudhvi Raj and Venkateswarlu, 2012).

3. Wavelet thresholding

Wavelet thresholding is a widely used term for wavelet domain denoising. Denoising by thresholding in wavelet domain has been developed principally by Donoho and Johnstone (1994) and Donoho (1995). In wavelet domain, large coefficients correspond to the signal, and small ones represent mostly noise. The denoised data are obtained by inverse-transforming the suitably thresholded, or shrunk coefficients.

Suppose $s = s_{i,j},\ i = \overline{1,M}$ and $j = \overline{1,N}$ is an image of $M \times N$ pixels, which is corrupted by independent and identically distributed (i.i.d.) zero mean, $n_{i,j}$ are independent standard normal $N(0,1)$ random variables and σ the noise level may be known or unknown. The noise signal can be denoted as $n_{i,j} \sim N(0,\sigma^2)$. This noise may corrupt the signal in a transmission channel. The observed, noise contaminated, image is $x = x_{i,j},\ i = \overline{1,M}$ and $j = \overline{1,N}$.

Therefore, the noised image can be expressed as:

$$x = s + \sigma n_{ij}. \tag{1}$$

The wavelet shrinkage denoising of signal $x(n)$, in order to recover $y(n)$ as an estimate of original signal $s(n)$ is represented as a 4-step algorithm (Taswell, 2000) with j representing decomposition levels, W is forward WT and W^{-1} is inverse WT.

1. $\omega_j = W(x)$, $j = 1$ to J.
2. $\lambda_j =$ Level adaptive threshold selection (ω_j).
3. $z_j =$ Thresholding(ω_j, λ_j).
4. $y = W^{-1}(z_j)$.

The standard thresholding of wavelet coefficients is governed mainly by either « *hard* » or « *soft* » thresholding function as shown in Fig. 2. The first function in Fig. 2a is a linear function, which is not useful for denoising, as it does not alter the coefficients. The linear characteristic is presented in the figure just for comparing the non-linearity of other two functions. The hard thresholding function is given as:

$$\begin{cases} z = hard(\omega) = \omega, & |\omega| > \lambda \\ z = hard(\omega) = 0, & |\omega| \leqslant \lambda \end{cases}, \tag{2}$$

where ω and z are the input and output wavelet coefficients respectively. $\lambda$is a threshold value selected.

Similarly, soft thresholding function is given as:

$$\begin{cases} z = soft(\omega) = \operatorname{sgn}(\omega)\max(|\omega| - \lambda, 0), & |\omega| > \lambda \\ z = soft(\omega) = 0, & |\omega| \leqslant \lambda \end{cases}. \tag{3}$$

Thresholding methods can be grouped into two categories, global thresholds and level dependent thresholds. The former method chooses a single value for threshold λ to be applied globally to all empirical wavelet coefficients while the latter method uses different thresholds for different levels. In this work, we have used the universal threshold, which is a simple entropy measure totally dependent on the size of the signal

$$\lambda = \sigma\sqrt{2\log(k)},$$

where k is the size of the signal and λ is the threshold value.These thresholds require an estimate of the noise level σ. The usual standard deviation of the data values is clearly not a good estimator (Ismail and Anjum Khan, 2012; Chang et al., 2000; Donoho, 1995), unless the underlying function S is reasonably flat. Donoho and Jhonstone considered estimating σ in the wavelet domain and suggested a robust estimate that is based only on the empirical wavelet coefficients at the finest resolution level. The reason for considering only the finest level is that the corresponding empirical wavelet coefficients tend to consist mostly of noise. Since there is some signal present even at this level, Donoho and Jhonstone proposed a robust estimate of the noise level σ based on the MAD (Median Absolute Deviation) (Naga Prudhvi Raj and Venkateswarlu, 2012), given by

$$\hat{\sigma}_{(\mathrm{MAD})} = \frac{median\{|x_{i,j}|\}}{0,6745}, \tag{4}$$

where $x_{i,j}$ represents the detail coefficients at the finest level.

4. Wiener filter and noise reduction

Wiener filter was adopted for filtering in the spectral domain. Wiener filter (a type of linear filter) is used for replacing the

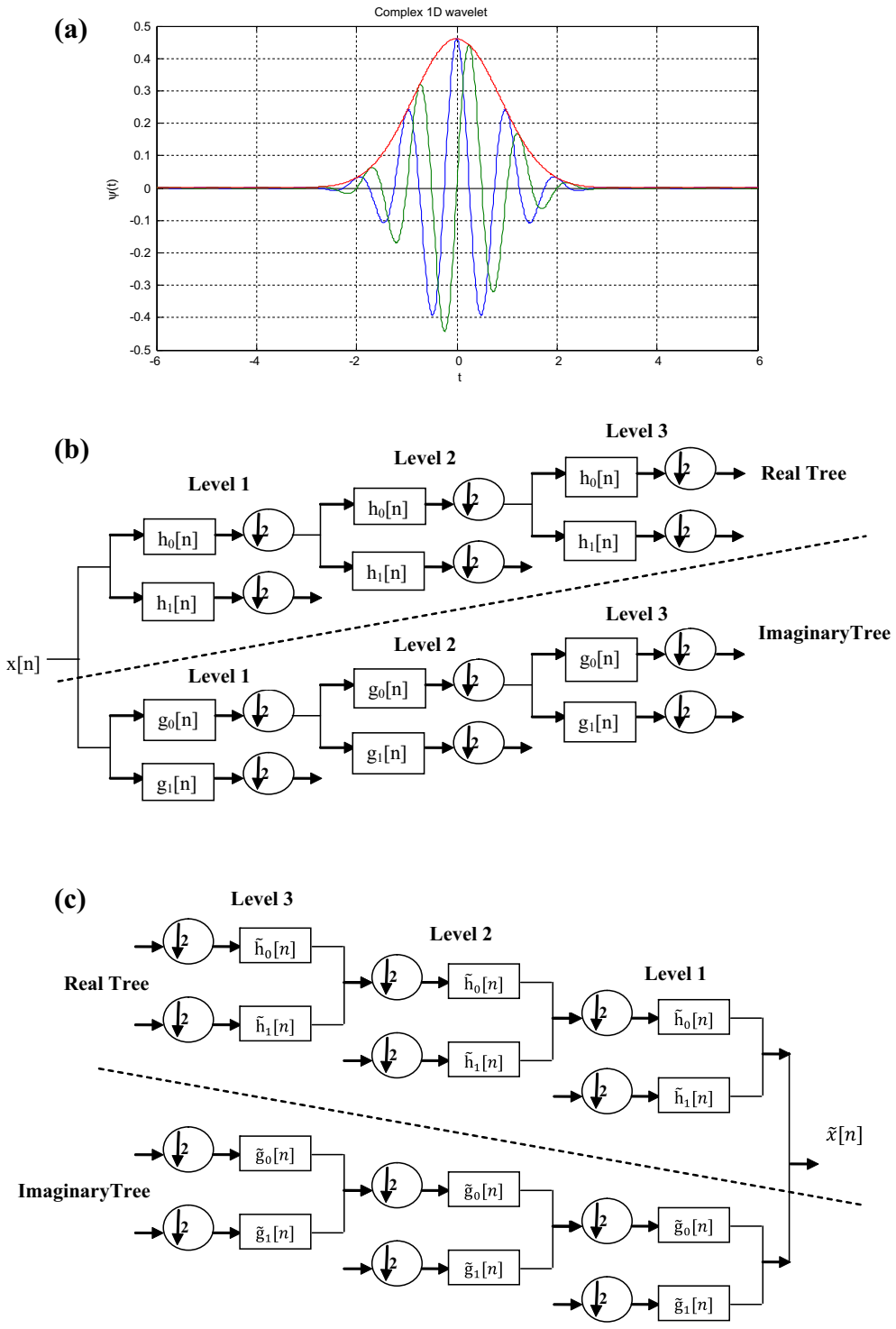

Figure 1 (a) 1D complex wavelet, (b) filter bank analysis for 1-D DTDWT,(c) synthesis filter bank for 1-D DTDWT.

FIR filter (Mitiche et al., 2013) to reduce noise in signal. When the image is blurred by a known low pass filter, it is possible to recover the image by inverse filtering. But inverse filtering is very sensitive to additive noise. The Wiener filtering executes an optimal trade-off between inverse filtering and noise smoothing. It removes the additive noise and inverts the blurring simultaneously (Kaur and Kaur, 2013; Asmaa Abass Ajwad, 2012). It minimizes the overall mean square error in the process of inverse filtering and noise smoothing. The Wiener filtering is a linear estimation of the original image. The approach is based on a stochastic framework. The orthogonality principle implies that the Wiener filter in Fourier domain can be expressed as follows:

$$W(f_1, f_2) = \frac{H^*(f_1, f_2) S_{xx}(f_1, f_2)}{|H(f_1, f_2)|^2 S_{xx}(f_1, f_2) + S_{\eta\eta}(f_1, f_2)}, \quad (5)$$

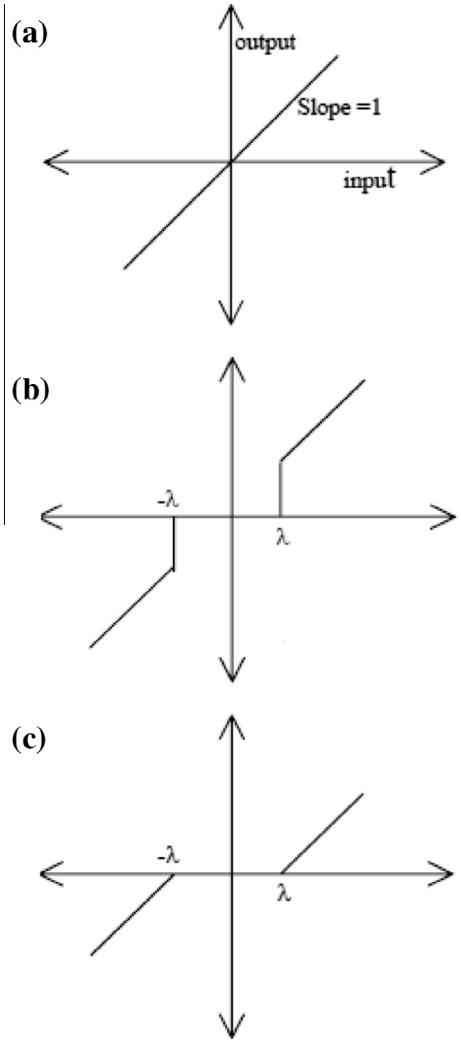

Figure 2 Thresholding functions: (a) linear, (b) hard, (c) soft.

where $S_{xx}(f_1, f_2)$,$S_{\eta\eta}(f_1, f_2)$ are respectively power spectra of the original image and the additive noise, and $H(f_1, f_2)$ is the blurring filter.

5. Experimental results

The aim of our comparison is to point out the differences in terms of PSNR (Peak Signal to Noise Ratio) due to a particular choice of wavelet bases. The PSNR has been computed using the following formula

$$\mathrm{PSNR} = 10\log_{10}\left(\frac{2^B - 1}{\sqrt{MSE}}\right). \tag{6}$$

The SSIM (Structural Similarity Index Measure) (Wang et al., 2004) is a perceptual measure that compares patterns of pixel intensities for images, on the basis of the local luminance and contrast of the analyzed pixels. Let x and y be two data vectors assumed to contain non-negative values only and representing the pixel values to be compared. The luminance and the contrast of these pixels are estimated by the mean and the standard deviation of x and y, respectively. The SSIM index between x and y is then given by

$$\mathrm{SSIM}(x, y) = \frac{(2\mu_x\mu_y + c_1)(2\sigma_{xy} + c_2)}{(\mu_x^2 + \mu_y^2 + c_1)(\sigma_x^2 + \sigma_y^2 + c_2)}, \tag{7}$$

where μ_x, $\mu_y$are the average of x, average of y ; σ_x^2, $\sigma_y^2$are the variance of x, variance of y, and $c_1 = (k_1 L)^2$, $c_2 = (k_2 L)^2$ are two variables to stabilize the division with weak denominator.

L is the dynamic range of the pixel-values (typically is $2^{Bbitsperpixel} - 1$), and $k_1 = 0.01$, $k_2 = 0.03$ (are taken by default).

The SSIM maps (Wang et al., 2007) indicate that the quality of the image by the proposed method is more uniformly distributed over the image space, and the resulting SSIM index map can be viewed as the quality map of the distorted images. Finally, a mean SSIM index of the quality map is used to evaluate the overall image quality.

The tabulation was made for σ vs PSNR and SSIM for DWT, SWT, DTCWT and DTCWT with Wiener filter and using both hard and soft thresholding functions as shown in Tables 1 and 2. The performance results of various algorithms can be evaluated for low and high noise conditions as follows:

- The denoising capability ($\sigma = 30$) of both DTCWT is better than SWT and DWT.
- Under high noise conditions ($\sigma = 300$), of both SWT, DWT and DTCWT give poor denoising results than even DTCWT with Wiener filter.

Table 1 Hard thresholding (PSNR and SSIM for various denoising methods with parameters $J = 3$, 'db4' family wavelets (Kharate et al., 2007)).

σ	DWT	SWT	DT-CWT	DT-CWT with Wiener filter
30	42.1516	43.2858	47.4061	44.7465
	0.8379	0.8718	0.9706	0.9629
50	37.0691	38.3027	46.0542	44.5527
	0.6569	0.7137	0.9605	0.9617
100	30.1486	31.4253	42.3218	43.7756
	0.3297	0.3883	0.916	0.9564
200	23.2199	24.5077	36.6588	41.6158
	0.1039	0.1305	0.7829	0.9357
300	19.1657	20.4557	32.8792	39.3308
	0.0443	0.0569	0.6446	0.9003

Table 2 Soft thresholding (PSNR and SSIM for various denoising methods with parameters $J = 3$, 'db4' family wavelets (Kharate et al., 2007)).

σ	DWT	SWT	DT-CWT	DT-CWT with Wiener filter
30	42.1517	43.286	46.3165	44.1177
	0.8379	0.8718	0.9649	0.9607
50	37.0693	38.3029	45.3018	43.9892
	0.6569	0.7137	0.9558	0.9601
100	30.1487	31.4255	42.1455	43.3846
	0.3297	0.3883	0.9138	0.9556
200	23.2199	24.5078	36.7922	41.4888
	0.1039	0.1305	0.7848	0.9356
300	19.1658	20.4558	33.0586	39.3438
	0.0443	0.0569	0.6484	0.9013

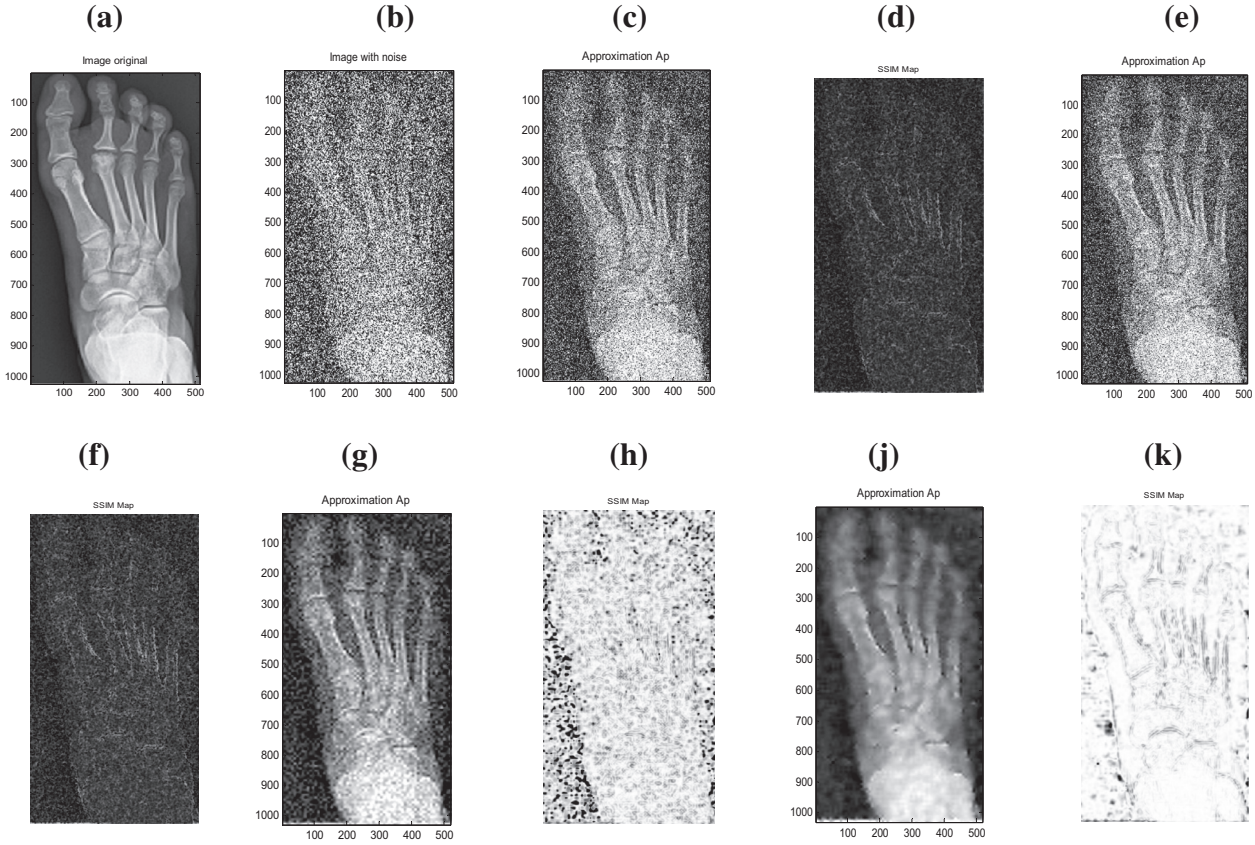

Figure 3 (a) Original image, (b) noisy image with $\sigma = 200$, (c) denoised image using DWT with soft threshold, (d) SSIM map for DWT with soft threshold, (e) denoised image with SWT with soft threshold, (f) SSIM map for SWT with soft threshold, (g) denoised image with DTCWT with soft threshold, (h) SSIM map for DTCWT with soft threshold, (j) denoised image with DTCWT–Wiener filter and the soft threshold, (k) SSIM map for DTCWT with wiener filter and with soft threshold.

We compare in Fig. 3, the reconstructed images obtained using DWT, SWT, DTCWT and DTCWT with Wiener filter for the medical image. It can be seen that the image for DTCWT with Wiener filter is better in preservation of many local structures and therefore presents the best quality of perceptual image. The visual quality improvement is also reflected in the corresponding SSIM maps, which provides useful guidance on how local image quality is improved over space. It can be observed from the SSIM map for DTCWT with Wiener filter that the areas which are relatively more structured benefit more obviously compared to the SSIM maps for DWT, SWT and DTCWT.

6. Conclusion

In this paper, denoising methods using universal threshold and the Wiener filter are applied for medical images. Firstly, we

estimate the image noise level. For the DWT, SWT and DTCWT based denoising we used the 'db4' family wavelets as a second step. Using the hard and the soft thresholding functions for the shrinkage of wavelet coefficients, their efficiency are compared in image denoising, based on PSNR (Peak Signal to Noise Ratio), SSIM (Structural Similarity Index Measure) and SSIM map.

References

Asmaa Abass Ajwad, 2012. Noise reduction of ultrasound image using wiener filtering and haar wavelet transform techniques. Diyala J. Med. 2 (1).

Chang, S.G., Yu, B., Vetterli, M., 2000. Adaptive wavelet thresholding for image denoising and compression. IEEE Trans. Image Proc. 9 (9), 1532–1546.

Donoho, D.L., 1995. Denoising by soft-thresholding. IEEE Trans. Inform. Theory 41 (3), 613–627.

Donoho, D.L., Johnstone, I.M., 1994. Ideal spatial adaptation via wavelet shrinkage. Biometrika 81 (3), 425–455.

Ismail, B., Anjum Khan, 2012. Image de-noising with a new threshold value using wavelets. J. Data Sci. 10, 259–270.

Kaur, Jaspreet, Kaur, Rajneet, 2013. Image denoising for speckle noise reduction in ultrasound images using dwt technique. IJAIEM 2 (6).

Kharate, G.K., Patil, F.V.H., Bhale, N.L., 2007. Selection of mother wavelet for image compression on basis of image. J. Multimedia 2 (6), 44–52.

Kingsbury, N.G., 1999. Image processing with complex wavelets. Philos. Trans. R. Soc. London A, Math. Phys. Sci. 357 (1760), 2543–2560.

Mitiche, Lahcène, Adamou-Mitiche, Amel Baha Houda, Naimi, Hilal, 2013. Medical image denoising using Dual Tree Complex Thresholding Wavelet Transform. In: Ibrahim, Al-Oqily (Ed.), 2013 IEEE Jordan Conference on Applied Electrical Engineering and Computing Technologies (AEECT), Amman, Jordan, December 3–5, 2013. IEEE Catalog Number: CFP1366P-PRT, ISBN: 978-1-4799-2305-2.

Naga Prudhvi Raj, V., Venkateswarlu, T., 2012. Denoising of medical images using dual tree complex wavelet transform. Proc. Technol. 4, 238–244, C3IT-2012.

Rangayyan, Rangaraj M., 2005. Biomedical Image Analysis. CRC Press.

Satheesh, S., Prasad, K., 2011. Medical image denoising using adaptive threshold based on contourlet transform. ACIJ 2 (2).

Selesnick, I.W., Baraniuk, R.G., Kingsbury, N.C., 2005. The dual-tree complex wavelet transform. IEEE Signal Process. Mag. 22 (6), 123–151.

Taswell, C., 2000. The what, how and why of wavelet shrinkage denoising. IEEE Comput. Sci. Eng. 2 (3), 12–19.

Wang, Z., Bovik, A.C., Sheikh, H.R., Simoncelli, E.P., 2004. Image quality assessment: from error visibility to structural similarity. IEEE Trans. Image Process. 13 (4), 600–612.

Zhou, Wang, Qiang, Li, Xinli, Shang. 2007. Perceptual image coding based on a maximum of minimal structural similarity criterion. In: IEEE Inter. Conf. Image Proc, San Antonio, TX, Sept. 16–19.